



Brookhaven  
National Laboratory

# Probing the Higgs self-coupling with $HH \rightarrow b\bar{b}l\bar{l} + \text{MET}$ final states at the LHC and beyond

Fatima Bendebba<sup>1</sup>, Elizabeth Borst<sup>2</sup>, Abraham Tishelman-Charny<sup>2</sup>

<sup>1</sup>Hassan II University of Casablanca (MA).

<sup>2</sup>Brookhaven National Laboratory (USA).

## 1 Introduction

Since the discovery of the Higgs boson by the ATLAS and CMS collaborations at the Large Hadron Collider (LHC) in 2012, intense efforts have been devoted by the particle physics community to studying its properties, and comparing them to the predictions of the Standard Model (SM), including the couplings of the Higgs boson to itself and to other particles. The Higgs self-coupling can be measured directly in the Higgs pair production (HH) process, and will provide insight into the nature of electroweak symmetry breaking. In the SM, the di-Higgs cross section in proton-proton collisions is very small. However, a wide range of beyond-the-SM models predict enhancements to the di-Higgs production rate, which motivates searching for di-Higgs production even now, when the SM cross section is too small to measure in the current LHC dataset. The HH to  $b\bar{b}l\bar{l}$  analysis investigates the decay of the Higgs-boson pair, in which one of the Higgs bosons decays to a b-quark pair (bb) and the other decays to  $WW^*$ ,  $ZZ^*$ , or  $\tau^+\tau^-$ , with in each case a final state with two b-quarks, two light leptons, and two neutrinos, assessed via missing transverse energy, using  $140 \text{ fb}^{-1}$  of proton-proton collisions at a center-of-mass energy of  $\sqrt{s} = 13 \text{ TeV}$  recorded by the ATLAS Experiment at the Large Hadron Collider (LHC). Its primary aim is to significantly enhance the sensitivity of the measurement of the non-resonant Higgs boson pair production, based on efficient lepton triggers and a precise analysis of the estimation of signal and background processes. The search results in an observed (expected) upper limit of 9.7 ( $16.2_{-5.3}^{+8.5}$ ) times the Standard Model prediction for the cross-section of non-resonant Higgs boson pair production at a 95% confidence level using full Run 2 data. The production of SM HH, though, is an extremely rare process, with an expectation of only around 4,000 events throughout the entire Run 2 operation - which corresponds to data collection from 2015 to 2018 -, compared with the production of a single Higgs boson estimated to be more than 8 million over the same period. The prospect of observing HH production and better constraining the Higgs boson self-coupling is expected to be improved at the LHC Run 3 and High-Luminosity LHC (HL-LHC) which plans to increase the peak luminosity of proton proton collisions by a factor of five compared to the Run 2 operation, and eventually deliver

3000  $fb^{-1}$  of integrated luminosity at  $\sqrt{s} = 14$  TeV. With this increased luminosity leading to radiation damage, and higher data rates, the current ATLAS tracking detector will become unusable for the HL-LHC. Therefore, ATLAS scientists are actively developing a new device called the Inner Tracker (ITk) to replace the current tracker. The ITk system is an all-silicon detector with a small-radius pixel detector and a multi-layer strip detector wrapped around it. The report is organized into two main sections: The first section is dedicated to the study of Higgs boson pair production, in particular in the  $bbll$  final state, where I will show the results obtained with the full run 2 data as well as the ongoing R&D efforts for this analysis with the ongoing Run 3 data collection. In the second section, I will highlight my involvement in the ITk project at BNL, focusing on the ITk Strip Detector module testing.

## 2 $HH \rightarrow bbl + MET$ : Results with full Run 2 data

The main two dominant Higgs boson pair production modes are gluon-gluon fusion (ggF) and vector-boson-fusion (VBF) which contribute to over 95% of the total production cross-section in the SM [1]. The di-Higgs to  $bbll$  analysis [1] was conducted with the full Run 2 data collected between 2015 and 2018 at the Large Hadron Collider (LHC).

Multiple channels are contributed to the  $bbll + MET$  final state:  $HH \rightarrow bbW(l\nu)W(l\nu)$ ,  $HH \rightarrow bb\tau(l)\tau(l)$ ,  $HH \rightarrow bbZ(l)Z(\nu\nu)$ , and  $HH \rightarrow bbZ(\nu\nu)$ , where lepton is whether electron or muon. Figure 1 shows the branching ratios of these different di-Higgs decay channels, assuming standard model (SM) Higgs boson with  $m_H = 125.09$  GeV.

	bb	WW	$\tau\tau$	ZZ	$\gamma\gamma$
bb	34%				
WW	25%	4.6%			
$\tau\tau$	7.3%	2.7%	0.39%		
ZZ	3.1%	1.1%	0.33%	0.069%	
$\gamma\gamma$	0.26%	0.10%	0.028%	0.012%	0.0005%

**Fig. 1:** Branching ratios of various  $HH$  decay channels. The  $b\bar{b}WW^*$ ,  $b\bar{b}ZZ^*$ ,  $b\bar{b}\tau^+\tau^-$  decay channels are indicated by the black circle.

The analysis strategy is based on different steps of the selections to have the final signal we are looking for. First, the events are selected based on a combination between single and di-lepton triggers, and have exactly two light opposite charge leptons with a minimum momentum transverse set at 9 GeV, passing Identification and Isolation working points criteria, and have exactly two b-tagged jets identified using the "DLr1" algorithm with 77% efficiency working point. In addition, to differentiate between the signal and control regions, several selections are applied based on di-lepton and di-b-jet masses. Furthermore, to separate rare signal events from the large amount of background event, different multivariate analysis discriminants (MVAs) are used.

Figure 2 shows the data and Monte Carlo (MC) agreement. A Deep Neural Network (DNN) and a Boosted Decision Tree (BDT) are used to classify the events into ggF (as shown in the right side of figure 2) and VBF (represented in the left side of figure 2) categories respectively. Major backgrounds coming from  $t\bar{t}$ ,  $Z+HF$ , and  $W_t$  are constrained in the control regions defined for the both categorizes.

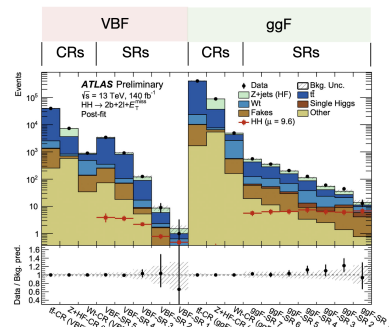


**Fig. 2:** Post-fit yields from the signal+background fit of the  $t\bar{t}$ ,  $Z+HF$ , and  $W_t$  control regions, both for the ggF and VBF event selections.

Overall, the  $bbll$  analysis with the full Run 2 data showed a huge improvement compared to the previous ATLAS search in this channel, with an observed (expected) 95% CL upper limit on the cross-section of di-Higgs production is set at 9.7 (16.2) times the SM prediction [1].

### 3 $HH \rightarrow b\bar{b}ll + MET$ : Ongoing R&D for Run 3 data

Following up on the exciting results from Run 2 data analysis, the  $HH$  to  $b\bar{b}ll + MET$  finale state analysis is getting ready for the Run 3 analysis phase, with ongoing research and development (R&D). As a first step, I started by exploring the potential of the use of a new ATLAS data format for our analysis in interest. For this reason, the  $HH$  production analysis adopts a new framework made to be adapted to these new files format. Within this framework, I am actively implementing the analysis package for the  $b\bar{b}ll$  analysis (see figure 3), including basic leptons and jet selections. The baseline  $b\bar{b}ll$  pre-selection, the kinematic variables, masses as well as the CutFlow checks have been successfully added to this framework.

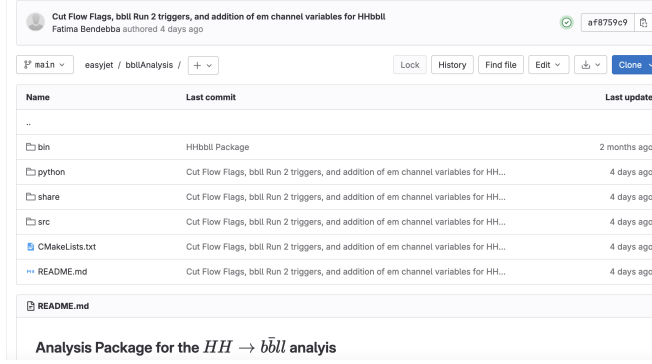


**Fig. 3:** The implementation of the analysis package for the  $HHb\bar{b}ll + MET$  analysis.

Figure 4 shows the CutFlow checks focusing on the non-resonant  $ggF$  signal considering one example for the  $b\bar{b}\tau^+\tau^-$  channel. The initial selections are listed as follows : Exactly two leptons ( $e^-$  or  $\mu^-$ ), events are selected based on a combination of the single-lepton and di-lepton triggers, exactly two light opposite charge leptons, and exactly two b-tagged jets. For the additional selections, we are considering two signal regions : SR1 is based on the di-lepton mass ( $15 \text{ GeV} < m_{ll} < 75 \text{ GeV}$  is set for same flavour leptons and  $15 \text{ GeV} < m_{ll} < 100 \text{ GeV}$  is set for different flavour leptons) and on a selection called VBFVeto which is considered as a region in the  $ggF$  analysis to reject as much as possible of the VBF events and simply defined as the reverse of the VBF event selections (Figure 4 a). SR2 is based on di-lepton and di-b-jet masses selections (Figure 4 b).

The Efficiency is defined as the number of events sequentially passing the selections mentioned previously, divided by the total number of events considered. The values highlighted in red correspond to the legacy Run 2 analysis, while those in black represent the new LHC data format for Run 3 data analysis. The results indicate a decrease in efficiency for both data formats, indicating a consistent behavior.

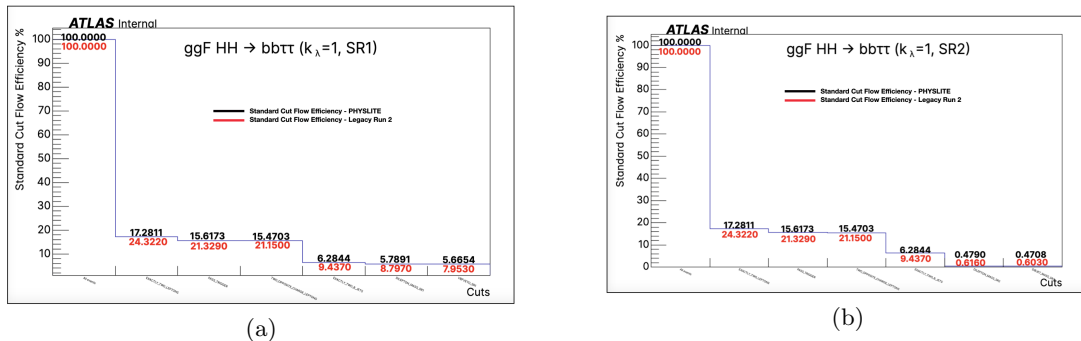


**Fig. 4:** The Standard CutFlow Efficiency for the  $b\bar{b}\tau^+\tau^-$  channel: (a) SR1 region, (b) SR2 region.

Furthermore, I have compared the shape of the di-lepton mass between these two different files formats for the different channels that contribute to this analysis as shown in the figure 5 which

shows clearly a good agreement.

In conclusion, the investigation strongly supports the adoption of the new LHC data format, affirming it as the correct direction to pursue.

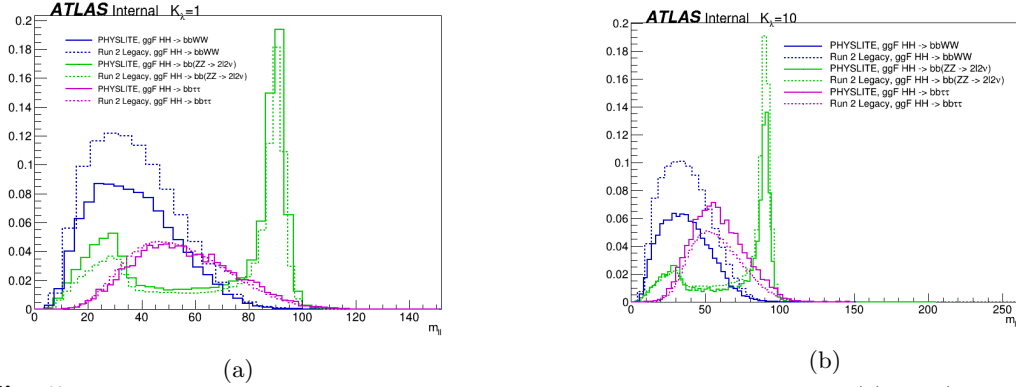


**Fig. 5:** The di-lepton mass distribution for the different HH decay channels: (a) SM ( $k_\lambda = 1$ ), (b) BSM ( $k_\lambda = 10$ ).

## 4 HL-LHC and ATLAS Inner Tracker (ITk)

### 4.1 HL-LHC Motivation

The standard model HH production cross section is too small to measure in the current LHC dataset. The high-luminosity (HL-LHC) [2] the upgrade to the LHC that is expected to be fully operational by 2029, plans to deliver an integrated luminosity of  $3000 fb^{-1}$  at  $\sqrt{s} = 14$  TeV, five times higher than that currently measured by ATLAS, which will significantly enhance the HH production that is anticipated to reach  $\sim 100,000$  events. However, this increased luminosity lead to so much radiation damage and higher data rates that the current ATLAS tracking detector will be unusable. For this reason, the current Inner detector will be replaced with a full-silicon Inner Tracker (ITK) consisting of a small-radius pixel detector and a large-area Strip tracking detector surrounding it. In this work I will focus on the ITK Strip detector [3].

### 4.2 ITk Strip Detector Overview

The ITK Strip detector consist of 392 staves, which are rectangular units with approximate area  $140 \times 10 cm^2$ . their essential role is to provide mechanical support for modules and provide space for the electrical, optical connections, and cooling services. Each stave contains 28 silicon-strip modules assembled on a carbon composite core. (Figure 6)

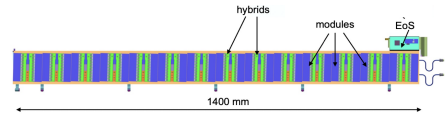


**Fig. 6:** Overview of the ITK Strip detector.

### 4.3 ITk Module Testing at BNL

Brookhaven National Laboratory (BNL) is responsible for testing the sub-detectors that makes up the strip ITK detector called **modules**. A module consists of a sensor, one power board, and hybrids that house up to 11 read-out ASICs. After modules assembly, each module passes through electrical and thermal quality control (QC) testing before progressing to the stave assembly step (Figure 7).

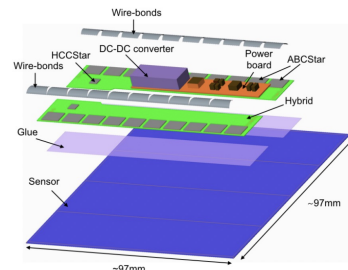


**Fig. 7:** Overview of the ITK Strip Modules.

In order to calibrate the timing mechanism on Module ASICs, ensure an uniform response of channels on ASICs and characterize noise, modules must be thermal-cycled 10 times from  $-35^{\circ}\text{C}$  to  $+20^{\circ}\text{C}$ . At both warm and cold temperatures, an electrical test (noise occupancy, gain) and IV (leakage current measured through the sensor as a function of the bias voltage) scan are performed to characterize the module electrically (Figure 8).

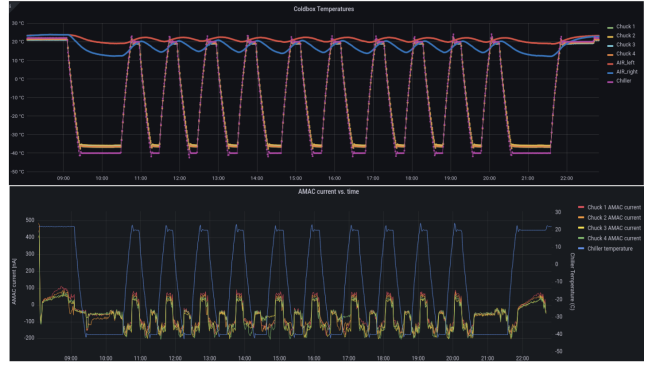


**Fig. 8:** Temperature and current measurements over time during module thermal cycling.

Figure 9 illustrates ITK Module testing results, figure 9 (a) shows the different between when the sensor is experiencing an early breakdown which is the case where this breakdown can prevent us to see the signal, or not. Electrical breakdown causes high leakage current in the sensor, which can lower a module’s signal to noise ratio. Figure 9 (b) the characterization of the noise, the top graph illustrates stable noise, while some strips in the bottom graph exhibit excessive noise

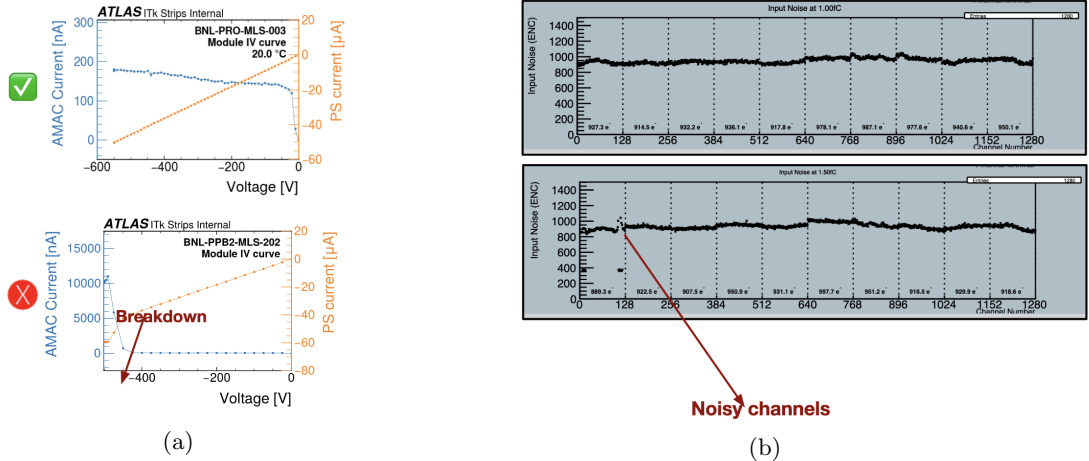


**Fig. 9:** A few module testing results. (a) IV test used to determine whether the sensor is experiencing an early electrical breakdown. (b) The characterization of noise in different channels on ASICs.

## 5 Conclusion

During Run 2 data analysis, I did some simulation work on the signal for the di-Higgs to  $b\bar{b}ll + MET$  analysis. Currently, ATLAS has begun the analysis for the LHC Run 3 data and in the search for  $HH$  to  $b\bar{b}ll + MET$ . I have contributed to an initial implementation of the  $b\bar{b}ll$  package in the new  $HH$  framework and I am exploring the use of a new ATLAS data format for the  $b\bar{b}ll$  search, by implementing the cutflow and studying the kinematics of the signal simulation. Regarding the high-luminosity LHC (HL-LHC), BNL optimizes the protocols used for an effective and efficient module testing after production and before stave assembly. Being part of this project at BNL has provided me with valuable experience in both hardware and software.

## References

- [1] ATLAS Collaboration, Search for non-resonant Higgs boson pair production in the  $2b + 2l + E_T^{miss}$  final state in pp collisions at  $\sqrt{s} = 13\text{TeV}$  with the ATLAS detector. CERN-EP-2023-233. [arXiv:2310.11286](https://arxiv.org/abs/2310.11286)
- [2] ATLAS Collaboration, Technical Design Report V. 0.1 for the High-Luminosity Large Hadron Collider (HL-LHC). CERN Yellow Reports: Monographs. CERN, Geneva, 2017. [http://cds.cern.ch/record/2284929](https://cds.cern.ch/record/2284929).
- [3] ATLAS Collaboration, Technical Design Report for the ATLAS Inner Tracker Strip Detector. Technical report, CERN, Geneva, Sep 2017. CERN-LHCC-2017-005, ATLAS-TDR-025 <https://cds.cern.ch/record/2257755>.